

Electronic supplementary information

Contents

Table S1 Calculated values of the shortest distance (r_s) between the benzene ring of phenol (PhOH) and hydrogen atoms of solvents of PhOH-(NH₃)_n ($n = 5-10$) in S₀.

Fig. S1-S6 Calculated structures of PhOH-(NH₃)_n ($n = 0-8$) in S₀ optimized at the M06-2X/cc-pVTZ level of theory.

Fig. S7-S10 Theoretical IR spectra in the mid-IR region for the PT and non-PT type structures of PhOH-(NH₃)_n ($n = 5-8$) in S₀ obtained at the M06-2X/cc-pVTZ level of theory.

Fig. S11 Pictures of normal mode vibrations for ν_{12} , ν_2 (NH₃ moiety), and ν_{9a} modes of the most stable isomer IXa of PhOH-(NH₃)₉ in S₀ calculated at the M06-2X/cc-pVTZ level.

Fig. S12 Comparison of experimental and theoretical IR spectra of PhOH-(NH₃)₉ in S₀ in the skeletal vibration region.

Table S1 Calculated values of the shortest distance (r_s) from the benzene ring of PhOH to hydrogen atoms of solvents of PhOH-(NH₃)_n ($n = 5-10$) in S₀. Values of the PT-type isomers are indicated by “PT” after the values. Values of structures that do not follow the threshold behavior are given in parentheses, see main text.

isomer	$r_s / \text{\AA}$	isomer	$r_s / \text{\AA}$	isomer	$r_s / \text{\AA}$	isomer	$r_s / \text{\AA}$	isomer	$r_s / \text{\AA}$	isomer	$r_s / \text{\AA}$
Va	2.70	VIa	2.59	VIIa	2.63	VIIIa	2.64	IXa	2.35 PT	Xa	2.30 PT
Vb	2.60	VIb	2.64	VIIb	2.65	VIIIb	2.73	IXb	2.66	Xb	2.32 PT
Vc	2.62	VIc	2.64	VIIc	2.63	VIIIc	2.63	IXc	2.28 PT	Xc	2.61
Vd	2.63	VId	2.68	VIIId	2.28 PT	VIIIId	2.25 PT	IXd	2.30 PT	Xd	2.51 PT
Ve	2.67	VIe	2.69	VIIe	2.63	VIIIe	2.31 PT	IXe	2.48 PT	Xe	2.63
Vf	2.70	VIIf	2.65	VIIIf	2.63	VIIIIf	2.25 PT	IXf	2.64	Xf	2.67
Vg	2.68	VIg	2.66	VIIg	2.66	VIIIg	2.45 PT	IXg	2.63	Xg	2.32 PT
Vh	2.71	VIh	2.71	VIIh	2.60	VIIIh	2.28 PT	IXh	2.59	Xh	2.51 PT
Vi	2.67	VIi	2.69	VIIi	2.61	VIIIi	2.45 PT	IXi	2.21 PT	Xi	2.32 PT
Vj	2.64	VIj	2.73	VIIj	2.34 PT	VIIIj	2.32 PT	IXj	2.72	Xj	2.52 PT
Vk	2.66	VIk	2.65	VIIk	2.34 PT	VIIIk	2.24 PT	IXk	2.69	Xk	2.33 PT
VI	(2.62 PT)	VII	2.66	VIII	(2.54)	VIII	2.68	IXl	2.29 PT	Xl	2.28 PT
		VIIm	2.79	VIIIm	2.22 PT	VIIIIm	2.62	IXm	2.25 PT	Xm	2.29 PT
		VIIn	2.62	VIIIn	2.49 PT	VIIIIn	2.26 PT	IXn	2.62	Xn	2.52 PT
		VIlo	2.21 PT	VIIlo	2.53 PT	VIIIlo	2.51 PT	IXo	2.34 PT	Xo	2.29 PT
		VIp	2.25 PT			VIIIp	2.26 PT	IXp	2.62		
		VIq	2.68			VIIIq	2.69	IXq	2.70		
		VIr	2.27 PT			VIIIr	2.35 PT	IXr	2.56 PT		
		VIIs	2.27 PT			VIIIs	2.63				
		VIIt	2.54 PT			VIIIIt	2.23 PT				
		VIlu	2.56 PT			VIIIlu	2.28 PT				
		VIv	2.43 PT								
		VIw	2.57 PT								
		VIx	(2.60 PT)								

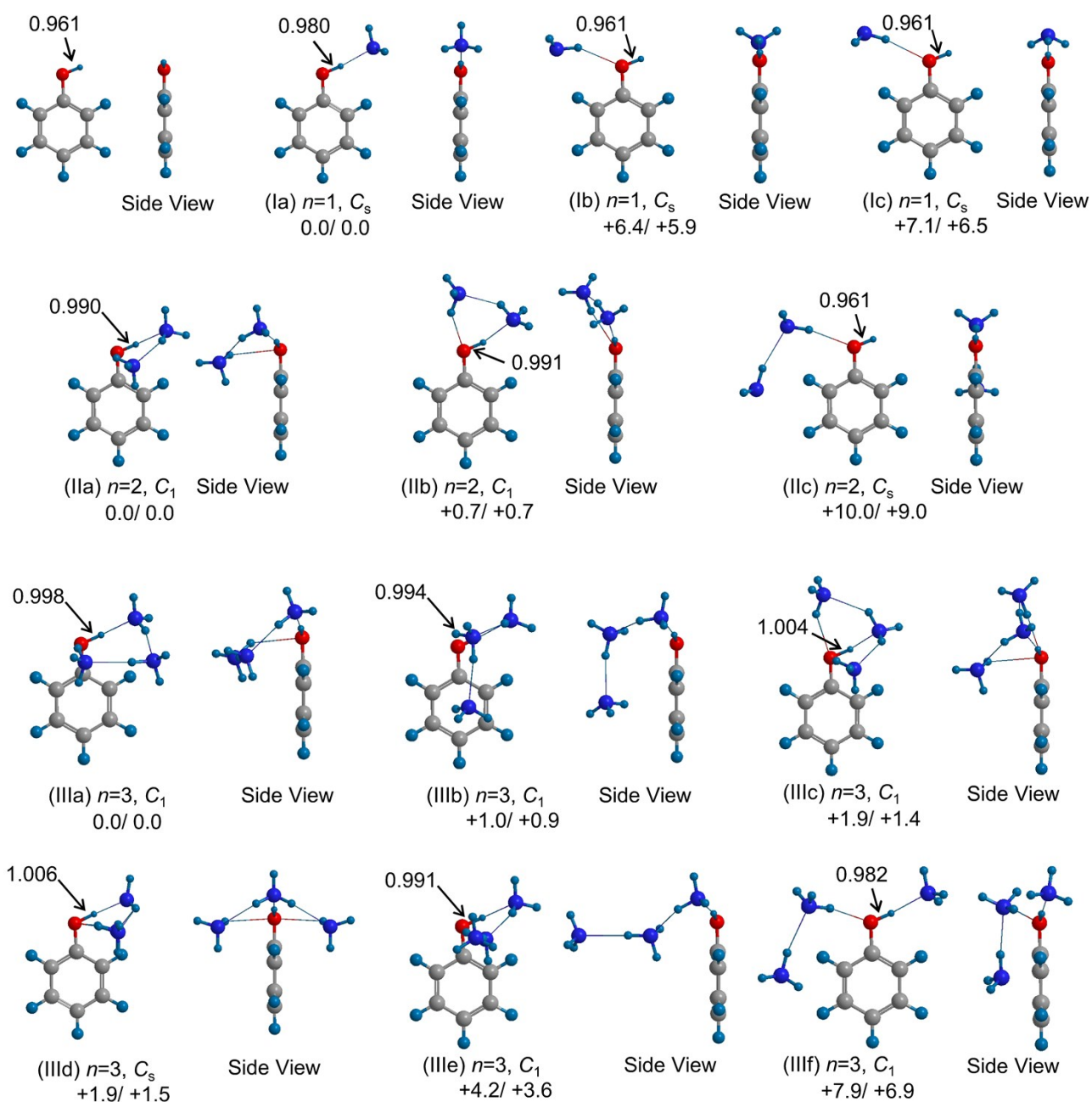


Fig. S1 Calculated structures of $\text{PhOH}-(\text{NH}_3)_n$ ($n = 0-3$) in S_0 optimized at the M06-2X/cc-pVTZ level of theory. The OH distances are given in Angstrom. Molecular symmetry and relative energies (kcal/mol) without and with the ZPE correction are given under each structure.

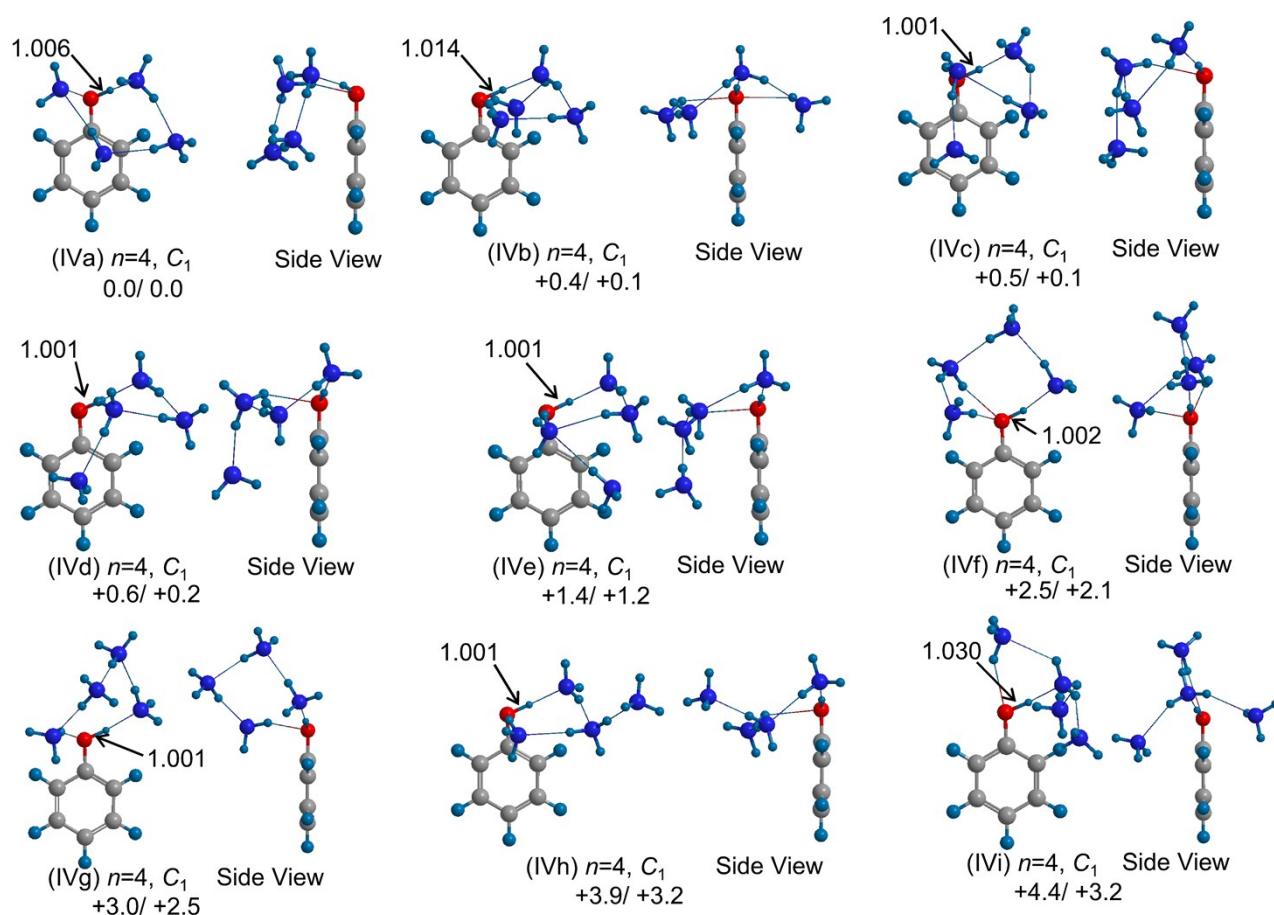


Fig. S2 Calculated structures of $\text{PhOH}-(\text{NH}_3)_4$ in S_0 optimized at the M06-2X/cc-pVTZ level of theory. The OH distances are given in Angstrom. Molecular symmetry and relative energies (kcal/mol) without and with the ZPE correction are given under each structure.

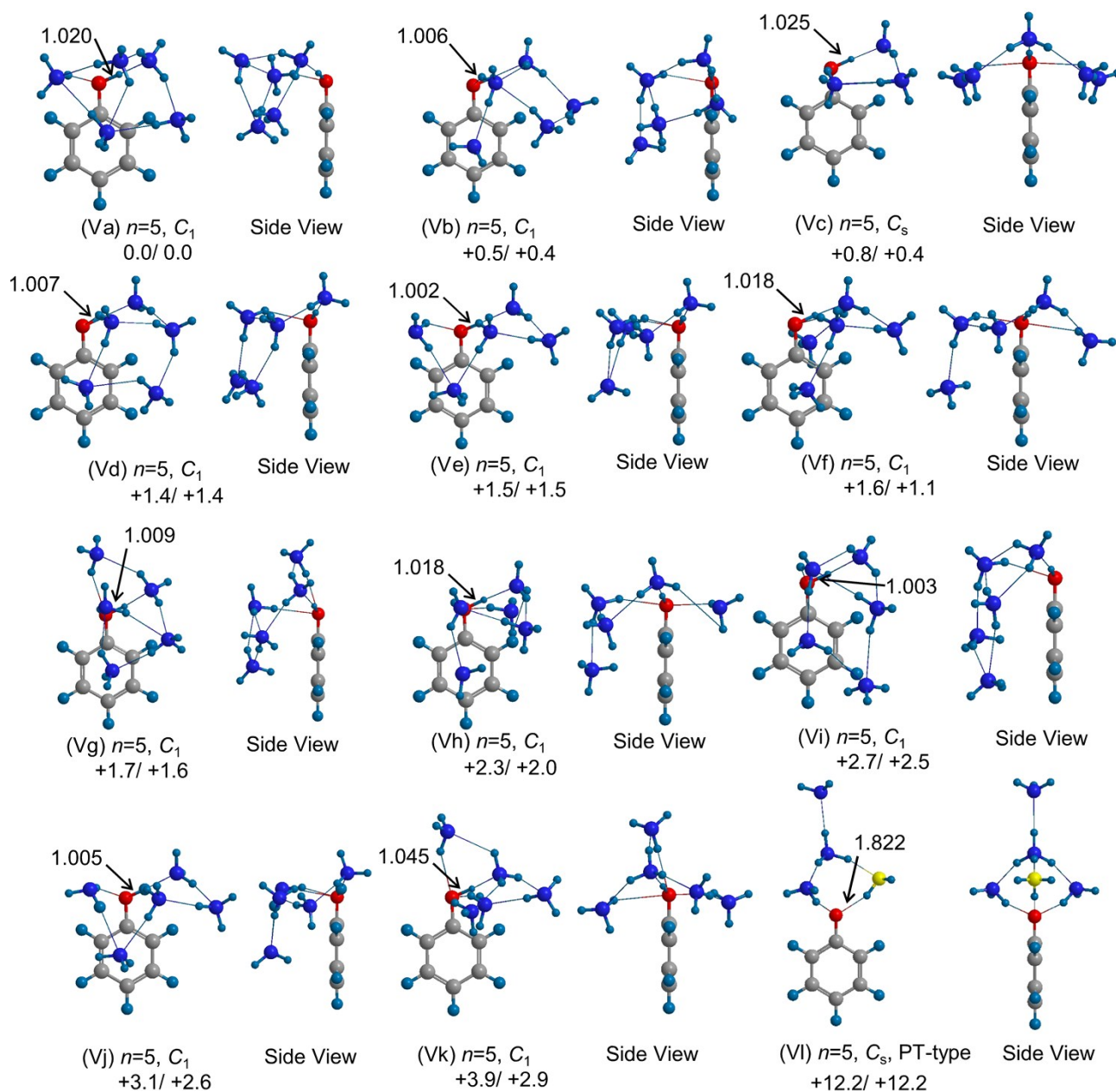
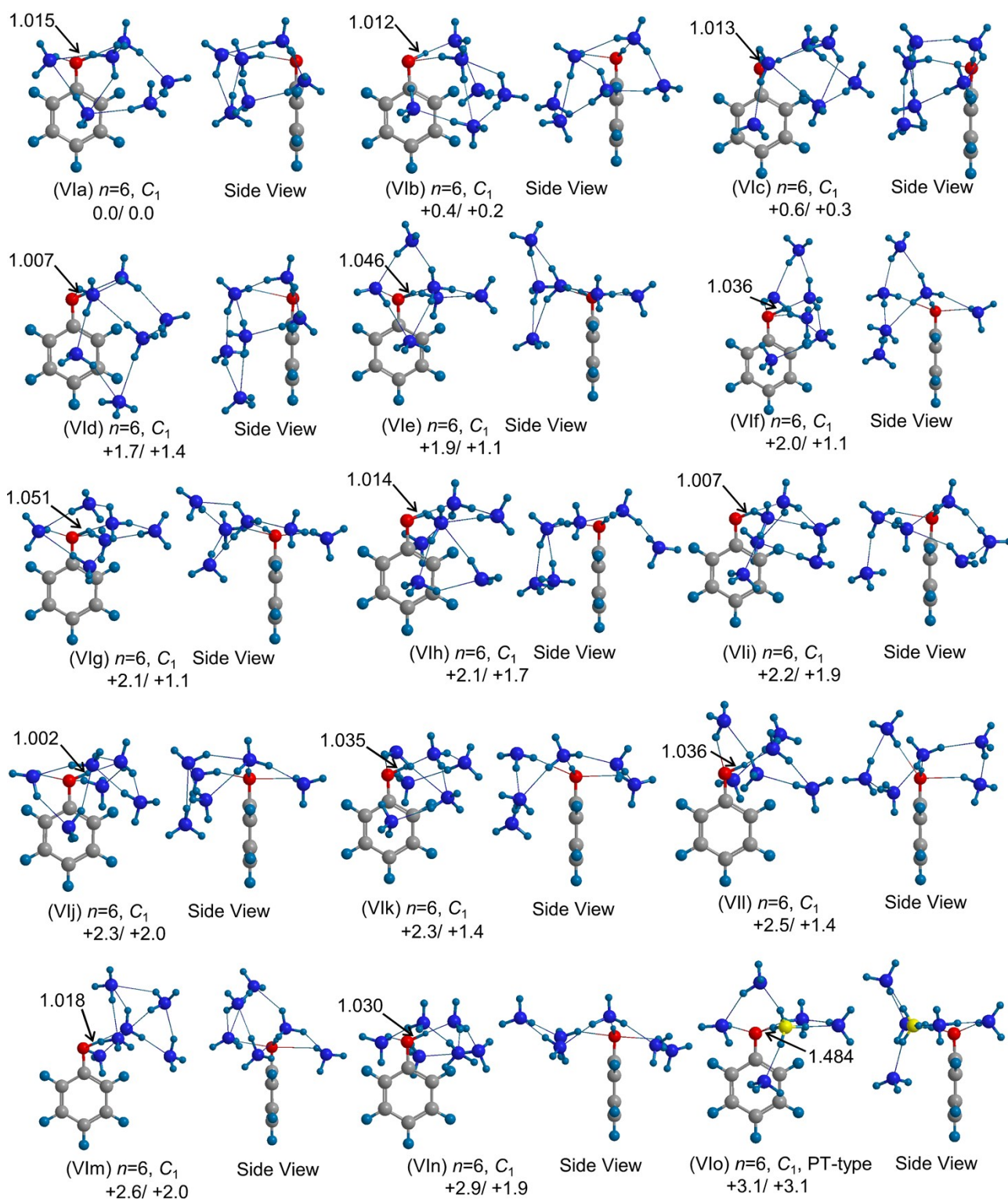


Fig. S3 Calculated structures of $\text{PhOH}-(\text{NH}_3)_5$ in S_0 optimized at the M06-2X/cc-pVTZ level of theory. The OH distances are given in Angstrom. Molecular symmetry and relative energies (kcal/mol) without and with the ZPE correction are given under each structure. The nitrogen atom of NH_4^+ in the PT type structures is marked yellow to distinguish it from NH_3 .



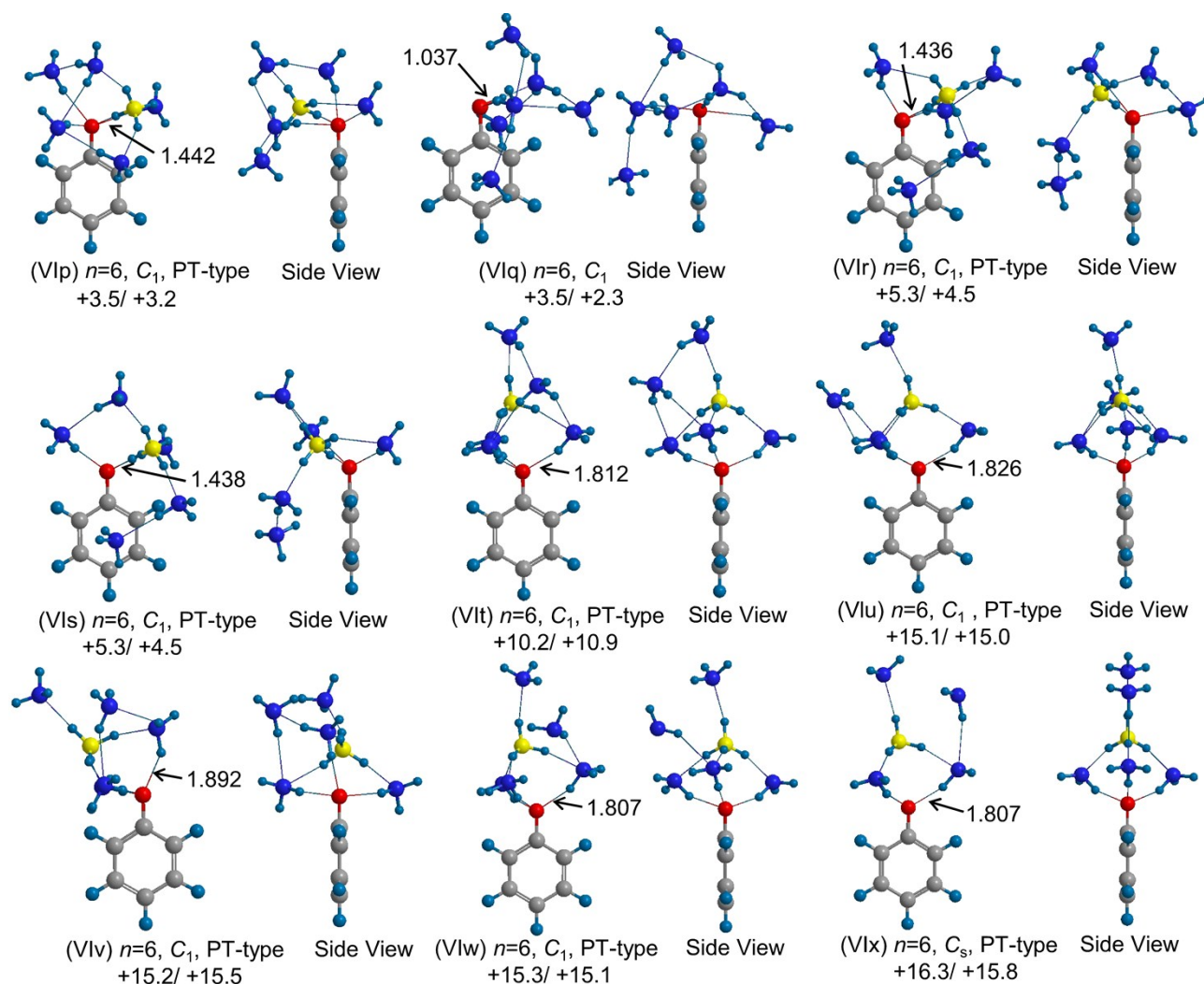


Fig. S4 Calculated structures of $\text{PhOH}-(\text{NH}_3)_6$ in S_0 optimized at the M06-2X/cc-pVTZ level of theory. The OH distances are given in angstrom. Molecular symmetry and relative energies (kcal/mol) without and with the ZPE correction are given under each structure. The nitrogen atom of NH_4^+ in the PT type structures is marked yellow to distinguish it from NH_3 .

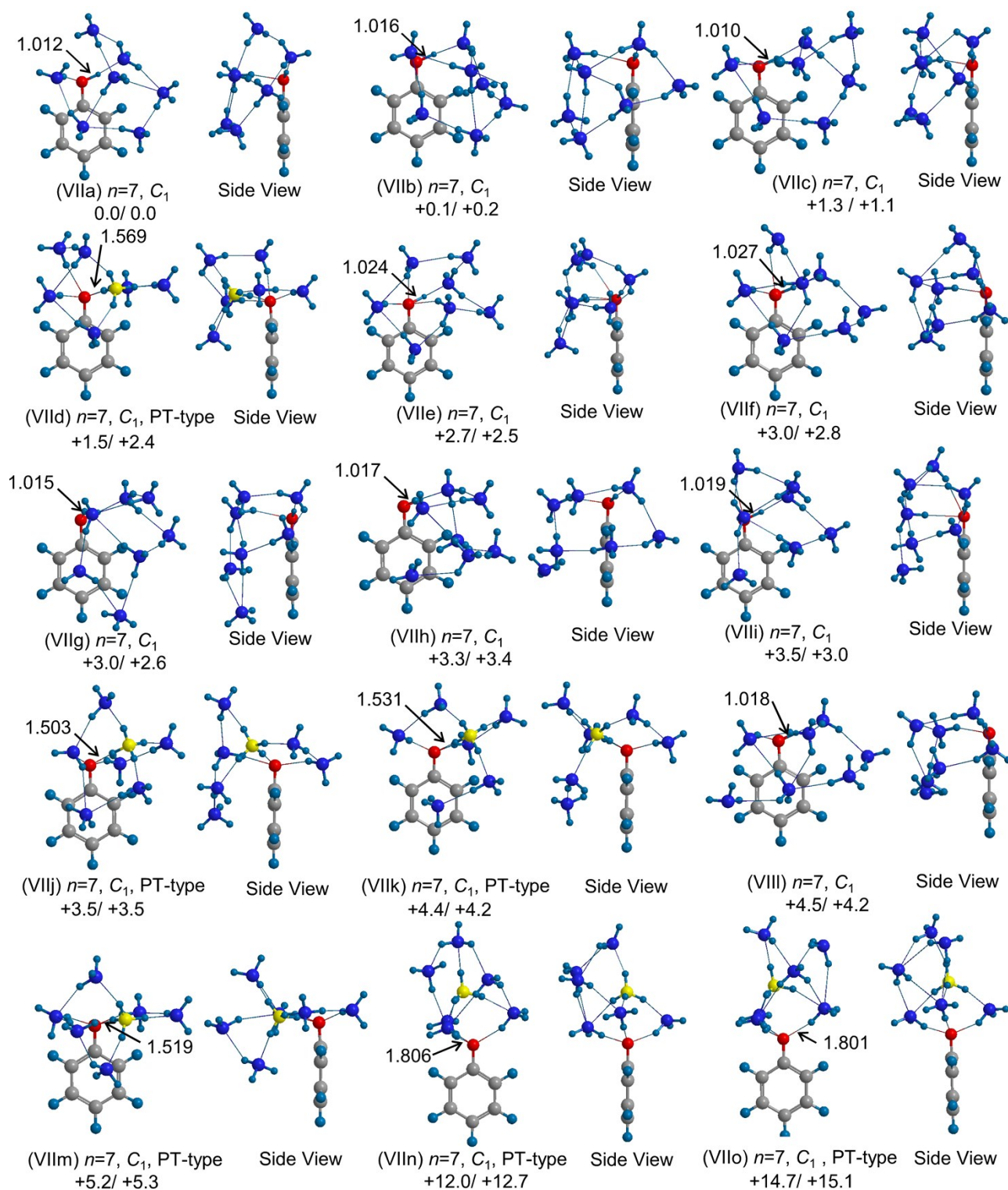
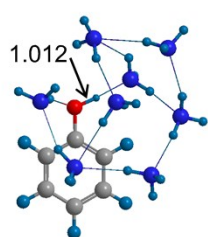
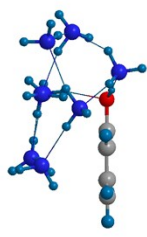


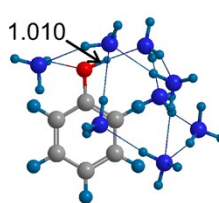
Fig. S5 Calculated structures of $\text{PhOH}-(\text{NH}_3)_7$ in S_0 optimized at the M06-2X/cc-pVTZ level of theory. The OH distances are given in angstrom. Molecular symmetry and relative energies (kcal/mol) without and with the ZPE correction are given under each structure. The nitrogen atom of NH_4^+ in the PT type structures is marked yellow to distinguish it from NH_3 .



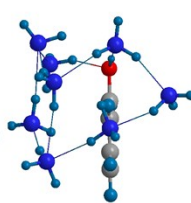
(VIIIa) $n=8$, C_1
0.0/ 0.0



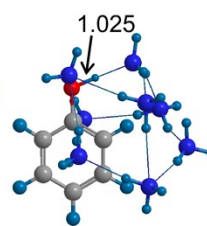
Side View



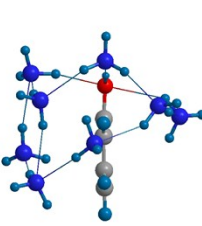
(VIIIb) $n=8$, C_1
+0.5 / +0.5



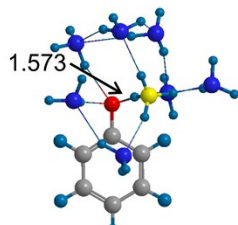
Side View



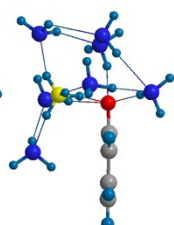
(VIIIc) $n=8$, C_1
+0.5/ +0.1



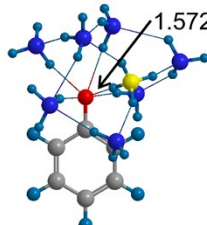
Side View



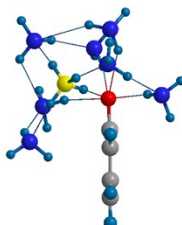
(VIId) $n=8$, C_1 , PT-type
+0.6/ +1.5



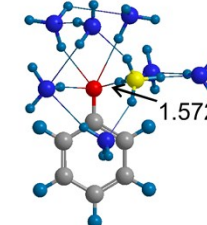
Side View



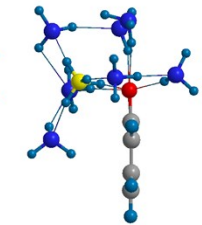
(VIIle) $n=8$, C_1 , PT-type
+1.1/ +1.7



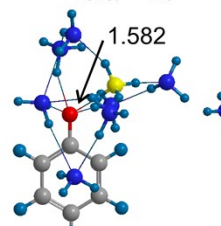
Side View



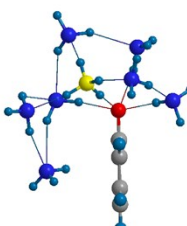
(VIIIf) $n=8$, C_1 , PT-type
+1.2/ +2.1



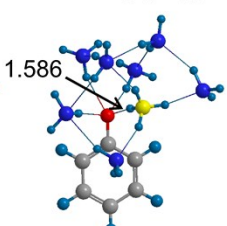
Side View



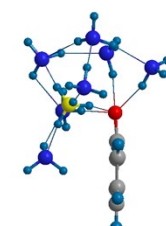
(VIIlg) $n=8$, C_1 , PT-type
+1.8/ +1.9



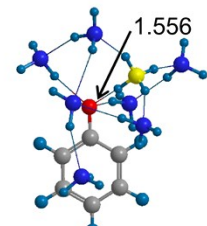
Side View



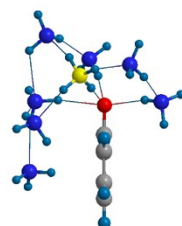
(VIIlh) $n=8$, C_1 , PT-type
+1.8/ +2.3



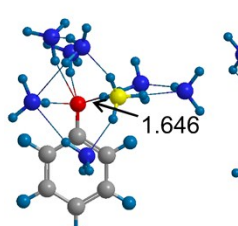
Side View



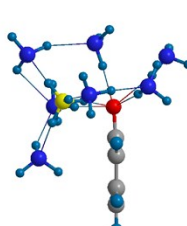
(VIIli) $n=8$, C_1 , PT-type
+2.2/ +2.1



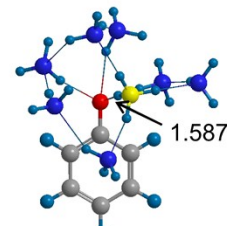
Side View



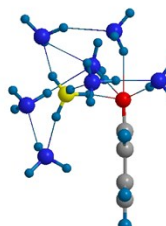
(VIIIj) $n=8$, C_1 , PT-type
+2.3/ +2.8



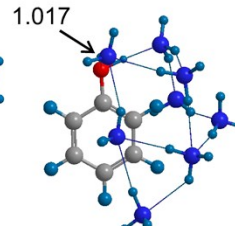
Side View



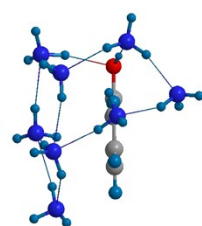
(VIIIk) $n=8$, C_1 , PT-type
+2.4/ +2.5



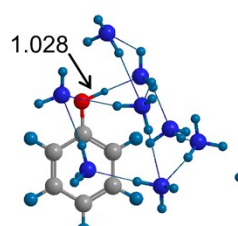
Side View



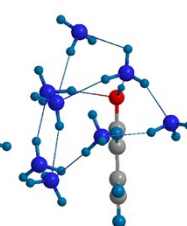
(VIIIl) $n=8$, C_1
+2.4/ +2.0



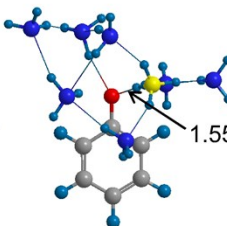
Side View



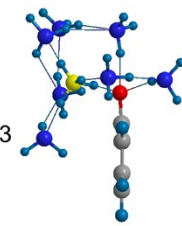
(VIIIm) $n=8$, C_1
+2.4/ +1.9



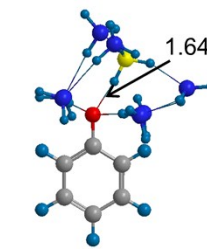
Side View



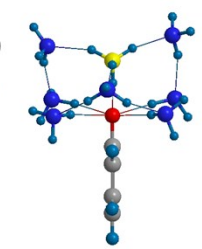
(VIIIn) $n=8$, C_1 , PT-type
+2.8/ +3.2



Side View



(VIIIo) $n=8$, C_1 , PT-type
+3.1/ +3.6



Side View

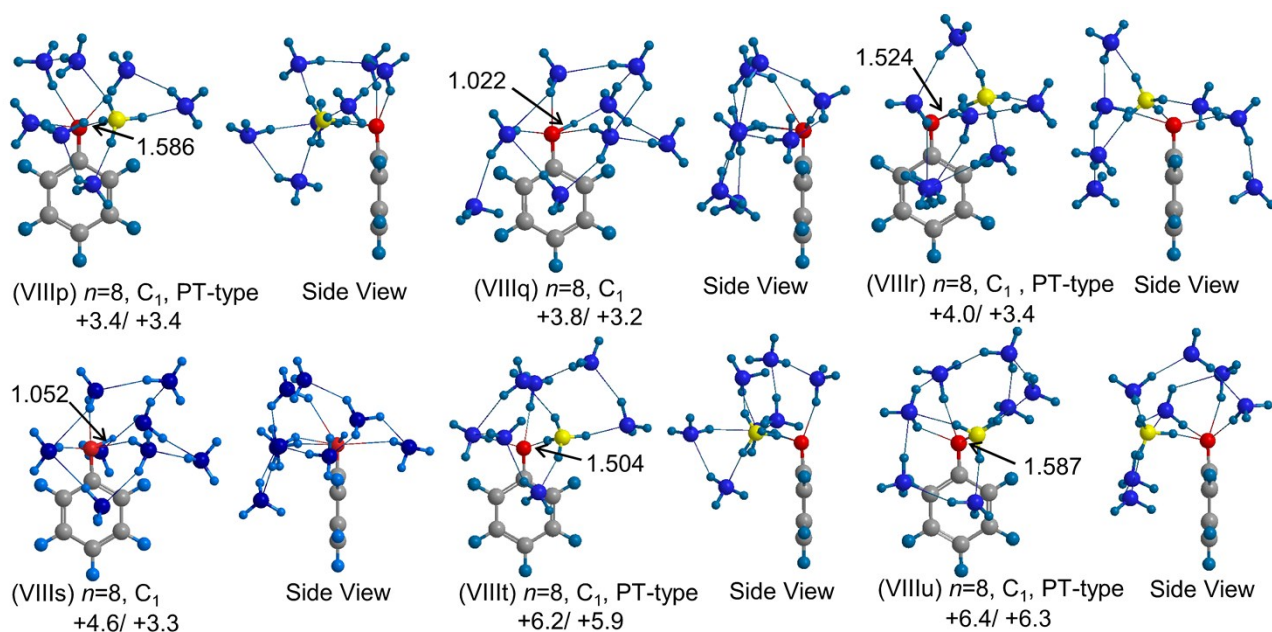


Fig. S6 Calculated structures of $\text{PhOH}-(\text{NH}_3)_8$ in S_0 optimized at the M06-2X/cc-pVTZ level of theory. The OH distances are given in angstrom. Molecular symmetry and relative energies (kcal/mol) without and with the ZPE correction are given under each structure. The nitrogen atom of NH_4^+ in the PT type structures is marked yellow to distinguish it from NH_3 .

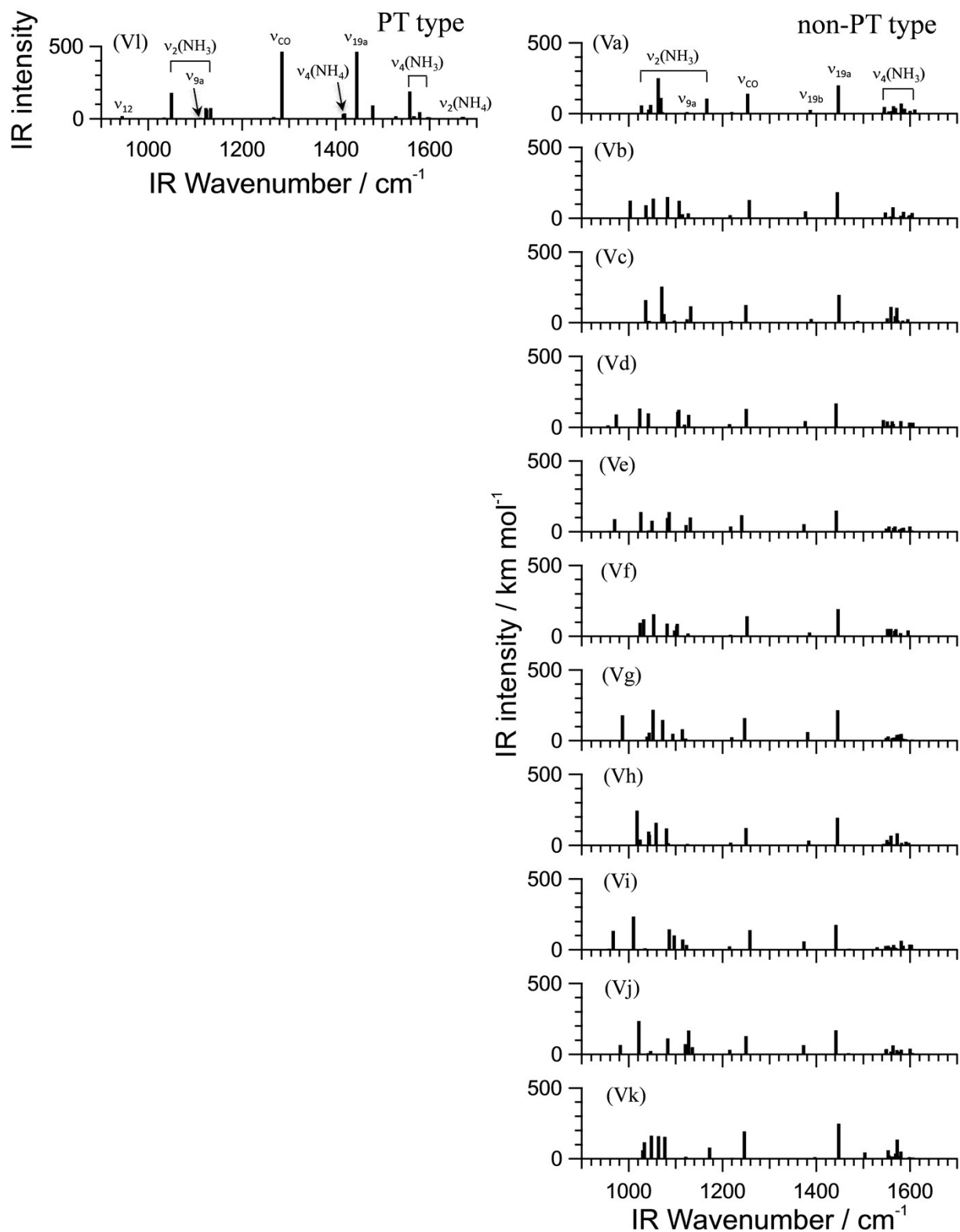


Fig. S7 Theoretical IR spectra for the PT and non-PT type structures of $\text{PhOH}-(\text{NH}_3)_5$ in S_0 obtained at the M06-2X/cc-pVTZ level of theory. The calculated vibrational frequencies have been scaled by 0.941.

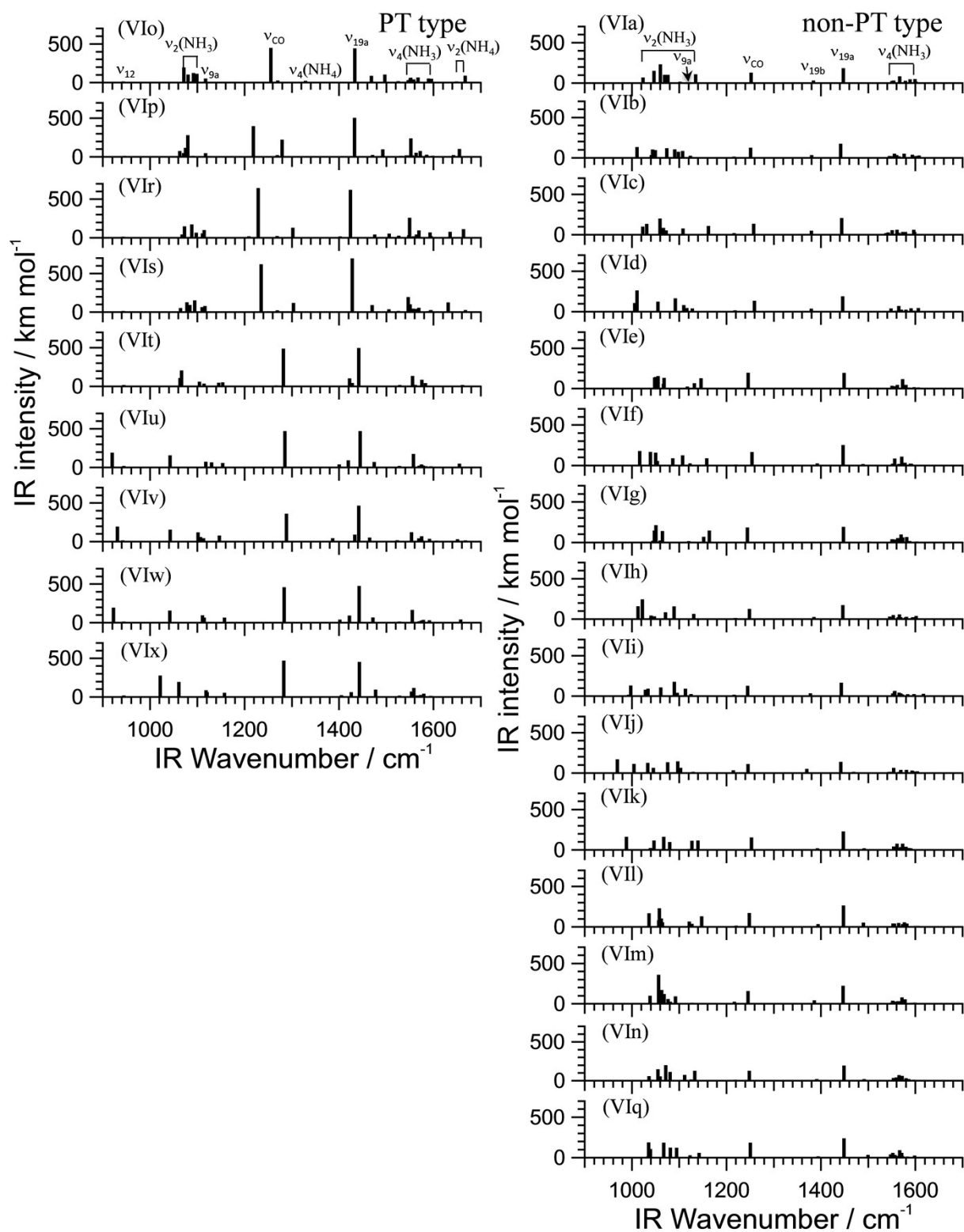


Fig. S8 Theoretical IR spectra for the PT and non-PT type structures of $\text{PhOH}-(\text{NH}_3)_6$ in S_0 obtained at the M06-2X/cc-pVTZ level of theory. The calculated vibrational frequencies have been scaled by 0.941.

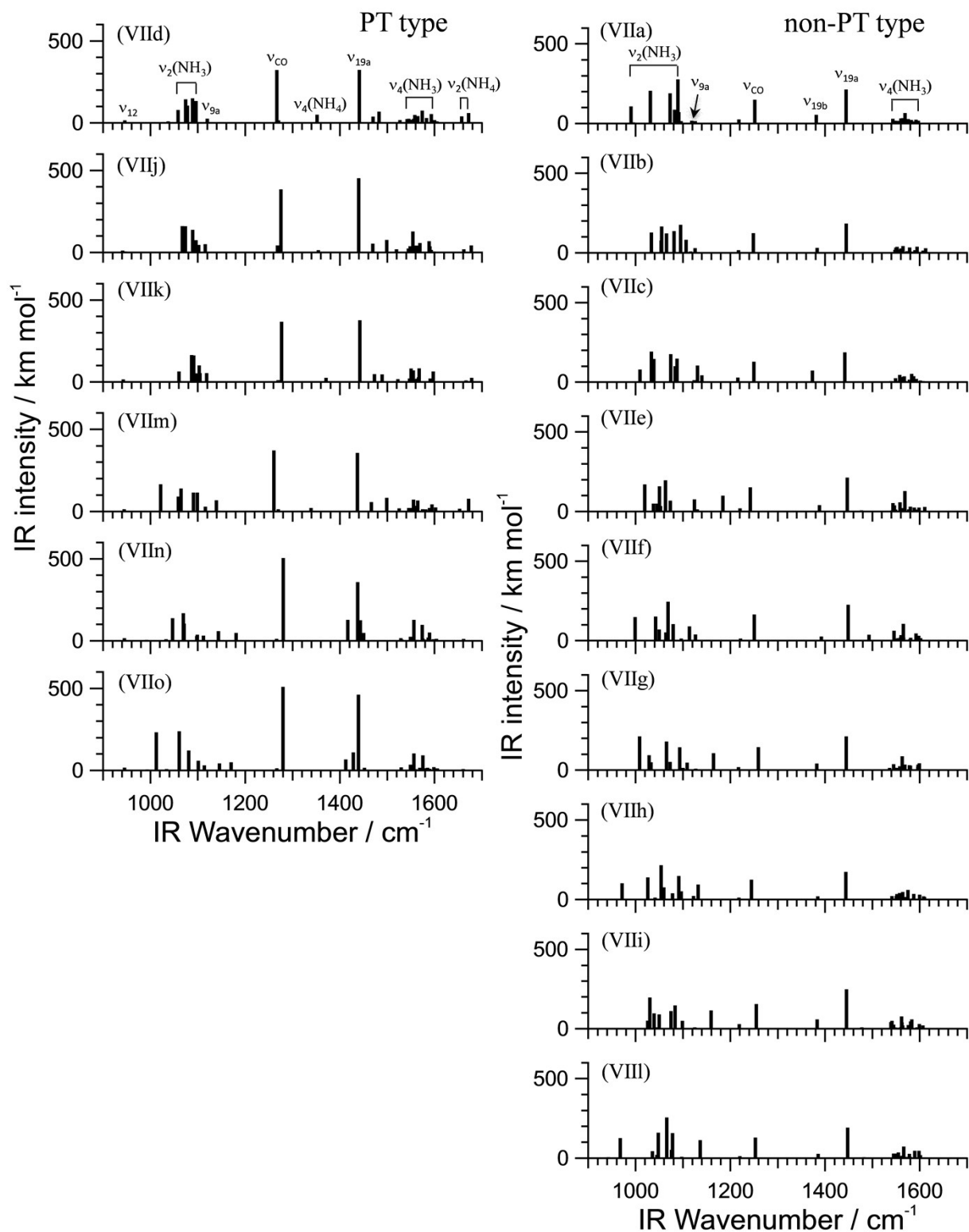


Fig. S9 Theoretical IR spectra for the PT and non-PT type structures of $\text{PhOH}-(\text{NH}_3)_7$ in S_0 obtained at the M06-2X/cc-pVTZ level of theory. The calculated vibrational frequencies have been scaled by 0.941.

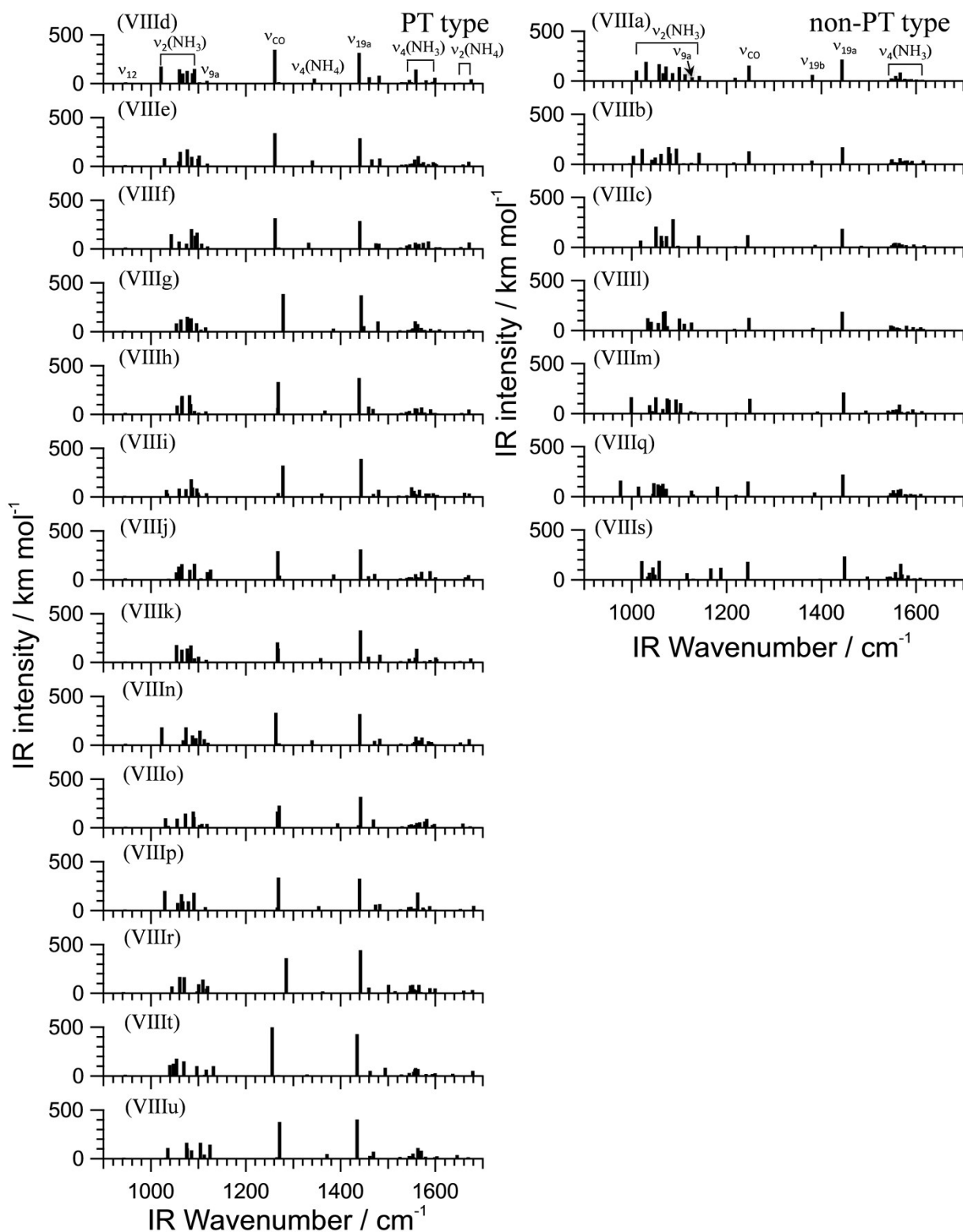


Fig. S10 Theoretical IR spectra for the PT and non-PT type structures of $\text{PhOH}-(\text{NH}_3)_8$ in S_0 obtained at the M06-2X/cc-pVTZ level of theory. The calculated vibrational frequencies have been scaled by 0.941.

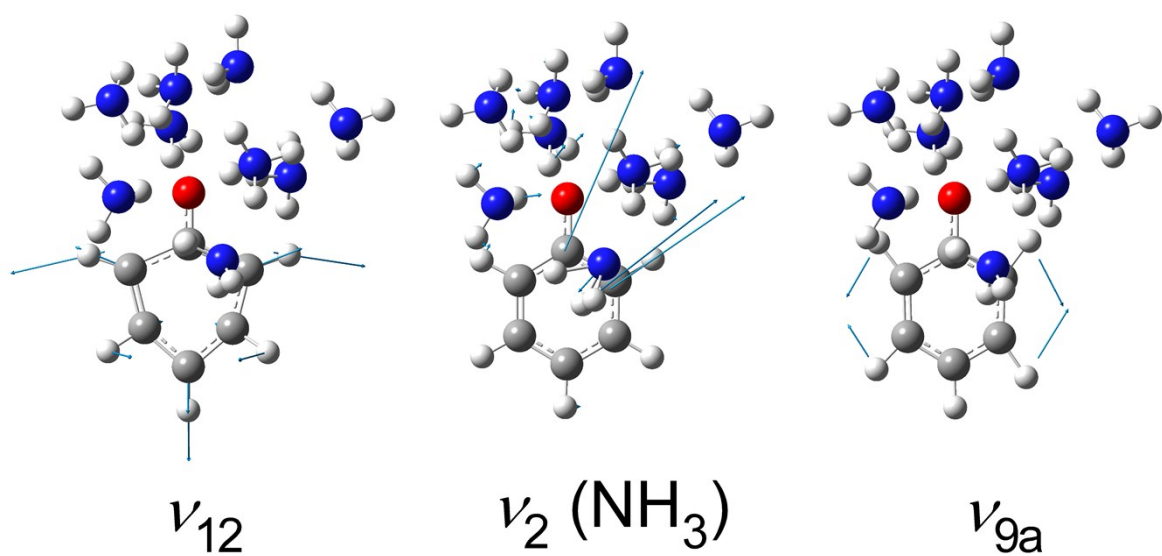


Fig. S11 Vibrational motions of ν_{12} , ν_2 (NH_3 moiety), and ν_{9a} modes of the most stable isomer IXa of $\text{PhOH}-(\text{NH}_3)_9$ in S_0 calculated at the M06-2X/cc-pVTZ level.

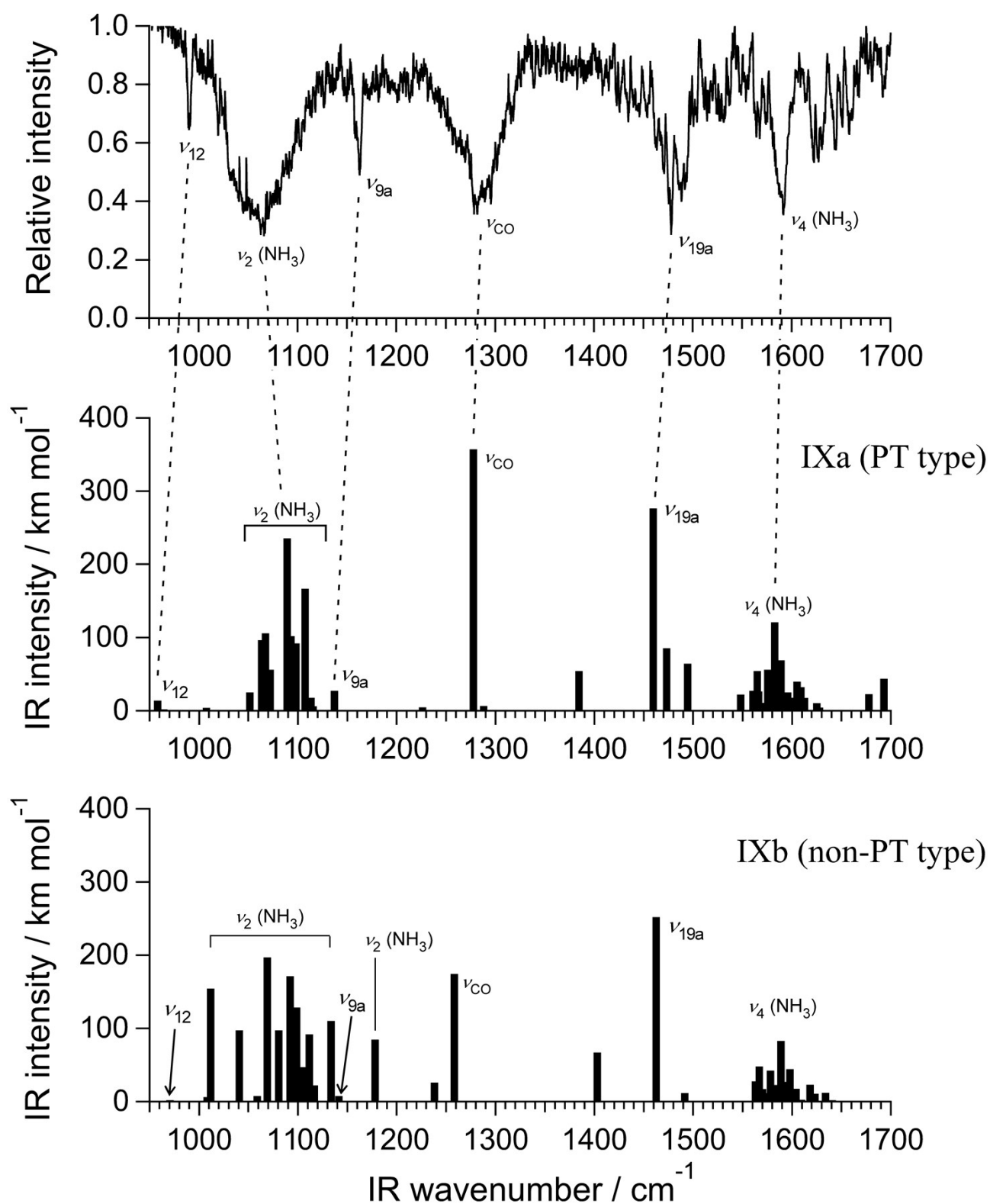


Fig. S12 Comparison of the experimental mid-IR spectrum with that of the most stable PT type cluster IXa and non-PT type cluster IXb of $\text{PhOH}-(\text{NH}_3)_9$ in S_0 obtained at the M06-2X/cc-pVTZ level of theory. The calculated vibrational frequencies have been scaled by 0.953.